BJR

Received: 8 February 2016 | Revised: 5 April 2016 | Accepted: 20 April 2016

http://dx.doi.org/10.1259/bjr.20160138

Cite this article as:
Chaudhari AJ, Ferrero A, Godinez F, Yang K, Shelton DK, Hunter JC, et al. High-resolution 18F-FDG PET/CT for assessing disease activity in rheumatoid and psoriatic arthritis: findings of a prospective pilot study. *Br J Radiol* 2016; **89**: 20160138.

FULL PAPER

High-resolution ^{18}F-FDG PET/CT for assessing disease activity in rheumatoid and psoriatic arthritis: findings of a prospective pilot study

[1]ABHIJIT J CHAUDHARI, PhD, [1,2]ANDREA FERRERO, PhD, [1]FELIPE GODINEZ, PhD, [1,3]KAI YANG, PhD, [1]DAVID K SHELTON, MD, [1]JOHN C HUNTER, MD, [4]STANLEY M NAGUWA, MD, [1]JOHN M BOONE, PhD, [4,5]SIBA P RAYCHAUDHURI, MD and [1]RAMSEY D BADAWI, PhD

[1]Department of Radiology, University of California Davis, Sacramento, CA, USA
[2]Department of Radiology, Mayo Clinic, Rochester, MN, USA
[3]Department of Radiology, Massachusetts General Hospital, Boston, MA, USA
[4]Department of Internal Medicine, University of California Davis, Sacramento, CA, USA
[5]Sacramento Veterans Affairs Medical Center, Rancho Cordova, CA, USA

Address correspondence to: Dr Abhijit J Chaudhari
E-mail: *ajchaudhari@ucdavis.edu*

Objective: Rheumatoid arthritis (RA) and psoriatic arthritis (PsA) commonly affect the small joints of the wrist and hand. We evaluated the performance of a new, high-resolution extremity positron emission tomography (PET)/CT scanner for characterizing and quantifying pathologies associated with the two arthritides in the wrist and hand joints.

Methods: Patients with RA or PsA underwent fluorine-18 fludeoxyglucose (^{18}F-FDG) PET/CT wrist and hand imaging, respectively, on the high-resolution scanner. Calibrated CT images and co-registered PET images were reconstructed. PET/CT was derived for the radiocarpal and pisiform–triquetral compartments, joints with erosive changes, sites of synovitis or tenosynovitis and the nail bed and were correlated with clinical and MRI findings.

Results: Significantly elevated ^{18}F-FDG uptake was measured for the radiocarpal and pisiform–triquetral compartments and at sites of bone erosion, synovitis, pannus and oedema, compared with unaffected joints ($p < 0.05$) in patients with RA, consistent with their clinical findings. In patients with PsA, significantly elevated ^{18}F-FDG uptake was measured for joints with synovitis compared with unaffected joints ($p < 0.05$), with patterns of ^{18}F-FDG uptake along the tendons, at the enthesis and in the nail bed, consistent with tenosynovitis, enthesitis and nail dystrophy, respectively.

Conclusion: High-resolution ^{18}F-FDG PET/CT imaging of the wrist and hand is feasible in an RA or PsA patient cohort and is capable of providing quantifiable measures of disease activity (synovitis, enthesitis, oedema and bone destruction).

Advances in knowledge: High-resolution PET/CT imaging shows promise as a tool for understanding the pathogenesis of the arthritic process and for non-invasive, objective assessment of RA or PsA severity and therapy selection.

INTRODUCTION

The pathogenesis of autoimmune inflammatory arthritis, such as rheumatoid arthritis (RA) or psoriatic arthritis (PsA), is a complex immune-mediated process.[1] Infiltration of activated immune cells (such as leukocytes) in joints is considered an early, crucial pathological event that initiates the inflammatory proliferative cascade, eventually leading to joint destruction. The activated immune cells secrete pro-inflammatory cytokines (tumour necrosis factor-α, interleukin-17 etc.) which significantly upregulate glucose metabolism in fibroblasts and activated macrophages[2,3] and contribute to the formation of bone-resorbing "pannus", a hallmark feature of the diseases.[4]

The positron emission tomography (PET) radiotracer fluorine-18 fludeoxyglucose (^{18}F-FDG)—a glucose analogue—is taken up by cells with elevated glucose utilization and is therefore particularly suited for imaging cells mounting an immune response in inflammatory arthritis.[5,6] ^{18}F-FDG PET is inherently quantitative, *i.e.* the signal intensity in the images relates directly to metabolic activity and provides an objective measure of the degree of metabolism, hence of inflammation.[7] In the context of RA, elevated ^{18}F-FDG uptake has been shown in large joints corresponding to synovitis,[5–7] bone marrow oedema[8] and inflammation.[9] X-ray CT presents a natural complement to PET, providing an anatomical reference to overlay and quantify the molecular images. CT also provides

direct information on pathological changes in the bone structure and composition, such as those observed in inflammatory arthritis.[10]

In RA and PsA, the small joints of the wrist and hand are considered early targets of the disease and provide a reasonable picture of disease progression.[11,12] Currently available whole-body PET/CT scanners—optimized for imaging large regions of the body—are suboptimal for quantifying radiotracer concentration (and hence, disease activity) for the small joints of the hand and wrist.[5,13] This is attributed to their relatively limited spatial resolution and resulting partial volume effect that limits quantification capability. Systems capable of limited-angle acquisition, such as the positron emission mammography Flex Solo II, also have a compromised ability for radiotracer activity quantification.[14]

A high-resolution extremity PET/CT scanner adaptable to wrist and hand imaging was built,[15] and its characterization in conditions typical for patient imaging was reported.[15,16] This system fully produces tomographic images with a spatial resolution of approximately 2.5 mm for the PET component and approximately 0.3 mm for the CT component. We report—employing prospective imaging data in human patients with established RA and PsA—the ability of this high-resolution PET/CT system to characterize and quantify disease activity and pathology associated with the two arthritides in the wrist and hand.

METHODS AND MATERIALS

Patient selection and characteristics

All procedures performed in studies involving human participants were in accordance with the ethical standards of the institutional research committee and with the 1964 Helsinki Declaration and its later amendments. Institutional review board approval and written informed patient consent were obtained for this prospective study. Eight patients (characteristics in Table 1) were recruited. Briefly, five patients had moderate-to-high RA disease activity based on the American College of Rheumatology criteria,[17] while three patients had active PsA based on the Classification Criteria for Psoriatic Arthritis[18] and Wright and Moll[19] criteria. Patients with uncontrolled diabetes, positive urine pregnancy test or who were breastfeeding were excluded from the study. Standard exclusion criteria were used for patients who also underwent MRI ($N = 3$) following the PET/CT scan. Physical examination [based on disease activity score 28 (DAS 28)[20]] was conducted within an average of 17 days before the scans by study rheumatologists. For the patients with RA, there is no standard for defining clinical positivity for the joints between the small bones of the wrist—the current clinical standards (*e.g.* DAS 28) define the wrist as a single joint in the assessment questionnaire. Therefore, the study rheumatologists evaluated swelling and tenderness using a single binary score for the entire wrist (1: yes, 0: no). For patients with PsA, the study rheumatologists evaluated eight joints: the proximal interphalangeal (PIP) joints 2–5 and the distal interphalangeal (DIP) joints 2–5, for swelling and tenderness using the binary score for each joint. Prior standard of care radiographs were obtained from the patient's electronic medical records.

Positron emission tomography/CT data acquisition

Patients fasted for at least 4 h prior to arriving for the study. A patient-specific immobilizer (fabrication time <5 min) was created for the most symptomatic hand to limit intrascan motion.[21] Patients received an i.v. injection of ^{18}F-FDG and rested quietly for 60 min in the University of California Davis Medical Center's radiotracer uptake rooms. The immobilizer was removed prior to patient injection and radiotracer uptake. Patients were then transported to the extremity PET/CT scanner, where scanning took place. Specifics regarding injected dose and uptake time are given in Table 1. Patient positioning on the extremity scanner is shown in Figure 1(a–c). The system has a field of view (FOV) of 12 cm in the coronal direction of the wrist. For patients with RA, the wrist was located by the immobilizer such that the FOV covered the region between the distal aspects of the radius and ulna and the distal aspects of metacarpals 2–5. For patients with PsA, the hand was located by the immobilizer such that the FOV covered the region between the proximal aspects of the proximal phalanges to the tip of the longest finger. A 12-min PET scan was conducted first, followed by a 16-s CT scan (80 kVp, 10 mA). CT images were reconstructed (Feldkamp method) in Hounsfield units with a voxel size of $0.38 \times 0.38 \times 0.28$ mm^3,[22] while the PET images were reconstructed (maximum *a posterori* method) with a voxel size of $1.1 \times 1.1 \times 3.3$ mm^3. PET image corrections were applied with the assistance of the co-registered CT[16] and images quantified in standardized uptake units were produced. Eligible

Table 1. Patient characteristics

Characteristic	All	RA	PsA
Number of patients	8	5	3
Age (years)	55.5 ± 6.7	55.0 ± 7.1	60 ± 4.6
Sex			
Male	4	1	3
Female	4	4	0
Injected dose (MBq)	374.9 ± 15.0	374.2 ± 17.0	376.2 ± 10.6
Uptake time (min)	83.1 ± 4.1	83.2 ± 4.8	83.0 ± 2.4
DAS 28	4.10 ± 0.84	3.87 ± 0.77	4.27 ± 0.93

DAS, disease activity score; PsA, psoriatic arthritis; RA, rheumatoid arthritis.
Data are expressed as mean ± standard deviation where relevant.

Figure 1. Patient positioning and the wrist immobilizer; (a) the subject is lying on the extremity positron emission tomography (PET)/CT system with the arm bent at the elbow inserted into the scanner bore through a hole in the table top; (b) the patient-specific wrist and hand immobilizer constructed from the thermoplastic material (white mesh), which attaches a custom-sized medical-grade styrofoam piece (light blue) by the means of nylon screws (visible locations demarcated by black dots); (c) the immobilizer inside the PET/CT gantry locked in place on the centre post by means of customized nylon stoppers. The PET and CT systems are rotated around the immobilized wrist and hand for image acquisition; and (d) the immobilizer is locked in a radiofrequency coil by a supporting apparatus that located the wrist and hand close to the isocentre of the coil. For colour image see online.

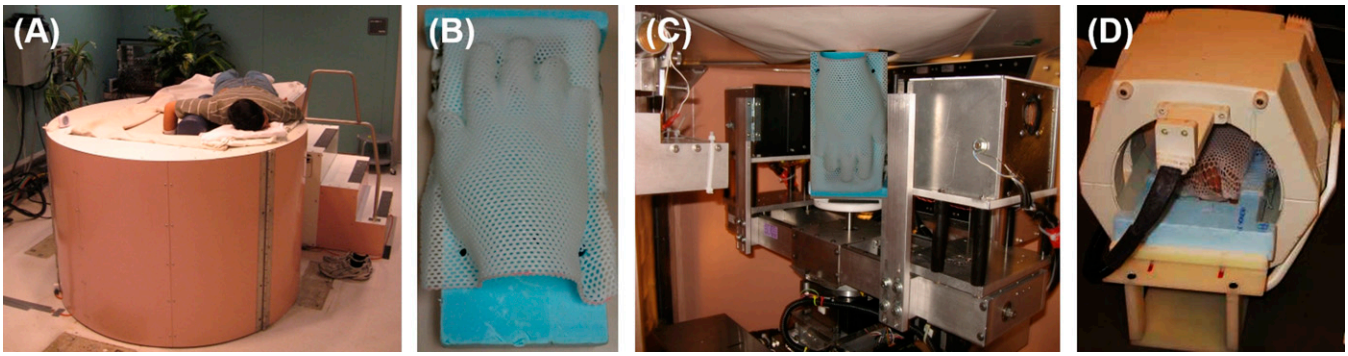

patients ($N = 3$) were transported to the MRI facility after PET/CT scanning.

MRI data acquisition

MRI scanning was carried out on a 1.5-T whole-body Signa Horizon MRI system (GE Healthcare, Inc., Waukesha, WI) using an extremity radiofrequency knee coil. The patients lay prone in the superman position with their symptomatic arm extended above the head into the radiofrequency coil. The patient-specific immobilizer aided in positioning the wrist close to the isocentre of the coil in the same orientation as the PET/CT scan for image co-registration (Figure 1(d)). Two sets of scans were conducted for most symptomatic wrists and hands:[1] a three-dimensional T_1 weighted (T1w) spoiled gradient-recalled echo sequence in both the coronal and axial direction (repetition time/echo time = 8.5/4.2 ms) with and without fat suppression and a two-dimensional short tau inversion recovery (STIR) sequence in the coronal direction (repetition time/echo time = 4000/20 ms, inversion time = 150 ms). In one subject, a power injector was used to inject the gadopentetate dimeglumine contrast agent at the rate of 1 ml s^{-1}. A single static T1w scan (same parameters as those for the T1w scan above, coronal direction, fat suppression on) was recorded at 4 min after the completion of contrast injection. The T1w images had a voxel size of $0.58 \times 0.58 \times 1\ mm^3$, while the STIR image had an in-plane resolution of $0.6 \times 0.6\ mm^2$, with a slice thickness of 3 mm.

Image processing and radiologic reading

Freehand regions of interest (ROIs) were manually placed by study radiologists on CT images at the following areas: patients with RA—the dorsal and volar radiocarpal compartments, the pisiform–triquetral compartment, the first carpometacarpal (CMC) joint and at sites of synovitis and bone erosions; patients with PsA—the PIP joints 2–5, the DIP joints 2–5 and the nail bed. For patients with RA, an ROI contained within the distal aspect of the radius served as an internal control, while an ROI contained within the third proximal phalange served as an internal control region for patients with PsA. The maximum standardized uptake value (SUV_{max}), as a surrogate for the degree of glucose metabolism, was measured for each ROI. For patients with RA, the metabolically active volume (MAV) was measured as the volume of tissue at the site of the ROI which had an intensity value >40% of the SUV_{max} of the ROI.[23] The MAV was considered an indicator of inflamed tissue volume. PET positivity, using the criteria described by Beckers et al,[5] was defined based on increased ^{18}F-FDG uptake by PET in areas corresponding to the joint synovium. For patients with RA, the wrist was considered PET positive when at least one wrist joint showed increased ^{18}F-FDG uptake on the scan. For patients with PsA, PET positivity was determined based on the same criteria[5] for each of the eight joints, namely the PIP joints 2–5 and the DIP joints 2–5, for each patient. A binary score was assigned to each joint, where 1 indicated a PET-positive joint and 0 indicated a PET-negative joint. The mean standardized uptake value (SUV) was determined for 24 asymptomatic joints (three joints per person) which had no history of RA, PsA or osteoarthritis (OA)-related symptoms or radiographic findings and did not show tenderness or swelling during the physical examination. The radiographs were read based on the Sharp/van der Heijde method for erosions and joint space narrowing,[24] while the first CMC OA was evaluated based on Eaton's method.[25] outcome measures in rheumatoid arthritis clinical trials (OMERACT) rheumatoid arthritis MRI scoring system (RAMRIS) scoring (v. 3)[26] was conducted from images of patients who underwent MRI. To determine the intraobserver and interobserver reliability for SUV_{max}, 2 study investigators drew freehand ROIs for the PIP joints 2–5 and the DIP joints 2–5 for the PET/CT scans of the 3 patients with PsA (24 joints in total). The ROI placement was repeated after a 1-week interval. Reliability was assessed using a two-way mixed, agreement-based, average-measures intraclass correlation coefficient (ICC).[27] A separate analysis for MAV was not performed, since that quantity is computed from the SUV_{max}.

Statistical analysis

All measures, unless otherwise specified, are given as mean ± standard deviation or median values, with relevant ranges where applicable. For the comparison of imaging measures, statistical significance was determined by one- or two-tailed Mann–Whitney U test ($p < 0.05$).

RESULTS

Fluorine-18 fludeoxyglucose positron emission tomography uptake in control regions and asymptomatic joints

The mean SUV in the ROIs used as internal control was 0.83 ± 0.32 (median = 0.75). The average SUV_{max} of these control ROIs was 0.89 ± 0.14 (median = 1.00). The average SUV_{max} of the asymptomatic joints (joints that did not present with swelling and tenderness during the clinical examination and those that did not show elevated ^{18}F-FDG uptake in the synovial region) was 1.12 ± 0.32 (median = 0.94). The difference between the SUV_{max} of the control ROIs and that of these asymptomatic joints was insignificant ($p = 0.14$, two-tailed test).

Fluorine-18 fludeoxyglucose positron emission tomography uptake in rheumatoid arthritis wrists

A representative CT and PET/CT image of a patient with RA is shown in Figure 2. All patients with RA had a DAS 28 > 3.0 and had at least one wrist joint that was PET positive; therefore, all evaluated wrists were considered PET positive for comparison with rheumatologic evaluation. The SUV_{max} and MAV results across RA wrists are summarized in Table 2. Table 3 summarizes the swelling, tenderness and PET positivity status for all five RA wrists. There was a perfect consistency between PET positivity and joint tenderness. Four wrists that presented with swelling were also PET positive; however, one wrist that was negative for swelling (but positive for tenderness) was PET positive based on the scan. Overall, however, there was a high consistency between PET positivity findings and wrist joint swelling.

Fluorine-18 fludeoxyglucose positron emission tomography uptake in the radiocarpal compartments in rheumatoid arthritis

^{18}F-FDG uptake was measured separately for the dorsal and volar radiocarpal compartments in patients with RA. A representative axial PET/CT image for a patient is shown in Figure 3(a). The SUV_{max} across all patients with RA in both the dorsal and volar compartments was significantly higher than that for the control joints ($p < 0.05$, one-tailed test). For the patient who received a contrast-enhanced MRI, there was a clear contrast agent accumulation in the dorsal radiocarpal compartment (Figure 4(a,b)). This region had an elevated ^{18}F-FDG uptake with SUV_{max} of 2.12 (Figure 4(d)). The co-registration between PET and MRI was accomplished *via* a pre-computed rigid registration between CT and MRI. The co-registered STIR image also showed fluid signals in the dorsal and volar aspects of the radiocarpal compartment (Figure 4(c)), possibly owing to oedema. Elevated ^{18}F-FDG uptake was measured in these areas. The contrast-enhanced and STIR images showed a high signal in the region of the first CMC joint and elevated ^{18}F-FDG uptake, consistent with the patient's first CMC OA, as we will discuss below.

Fluorine-18 fludeoxyglucose positron emission tomography uptake in the pisiform–triquetral compartment in rheumatoid arthritis

The SUV_{max} and MAV results for the pisiform–triquetral compartment in patients with RA are summarized in Table 2. Figure 3(b) shows a representative PET/CT image of a patient with RA with pronounced ^{18}F-FDG uptake in this compartment. Erosive changes on the apposing surfaces of the pisiform and triquetrum were also visualized from the underlying CT image. The SUV_{max} in this compartment across all patients with RA was statistically higher than the SUV_{max} measured for the control joints ($p < 0.05$, one-tailed test).

Fluorine-18 fludeoxyglucose positron emission tomography uptake at sites of erosion

All patients with RA presented with one or more carpal bone erosions on their prior radiographs. Figure 5 shows representative images of a patient with RA, indicating sites of erosive changes and associated synovitis. A STIR image is also shown for comparison demonstrating oedematous areas at sites of bone erosion. The SUV_{max} and MAV across all erosions in each patient with RA were computed and are summarized in Table 2. The SUV_{max} for ^{18}F-FDG uptake for erosions across all patients with

Figure 2. Extremity positron emission tomography (PET)/CT of a patient with rheumatoid arthritis; the coronal section showing a volar view of the right wrist from the (a) CT and (b) PET/CT overlay. Arrows show sites of bone erosion and corresponding fluorine-18 fludeoxyglucose (^{18}F-FDG) uptake (blue and light blue arrows) [maximum standardized uptake value (SUV_{max}) = 2.2], ^{18}F-FDG uptake in the pisiform–triquetral compartment (green arrows) (SUV_{max} = 1.89) and ^{18}F-FDG uptake at the first carpometacarpal joint (white arrows) (SUV_{max} = 5.50). The linear range of the PET colour scale shown is 18–45% of the SUV_{max}. For colour image see online.

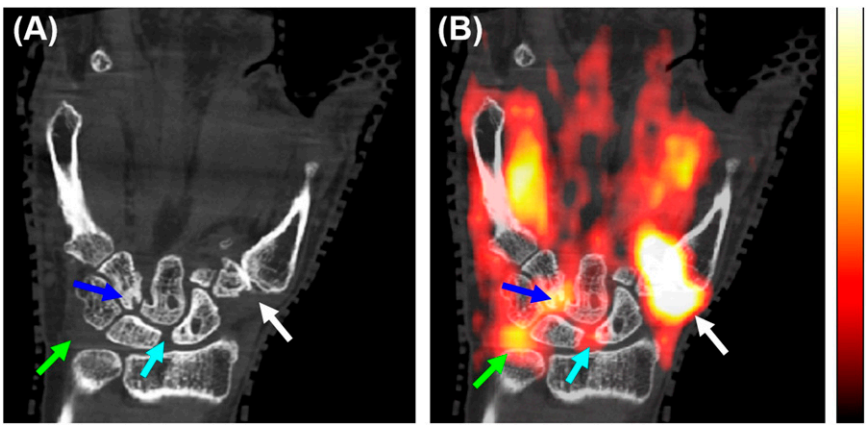

Table 2. Maximum standardized uptake value (SUV_{max}) and metabolically active volume (MAV) expressed as median (range) for the regions of interest in patients with rheumatoid arthritis (RA). All the wrists analyzed were positron emission tomography positive (Table 3)

Anatomical locations	SUV_{max}	MAV (cm^3)
Radiocarpal compartment		
Dorsal	2.11 (1.37–3.68)	3.68 (2.30–5.77)
Volar	1.67 (1.08–3.91)	3.23 (1.67–4.52)
Pisiform–triquetral compartment	1.89 (0.93–3.80)	1.46 (0.48–3.80)
Sites of RA erosions	2.20 (1.2–3.22)	2.77 (1.37–3.68)
First CMC joint	1.97 (0.98–5.50)	2.72 (1.97–6.81)

CMC, carpometacarpal.

RA was significantly higher than that of the control joints ($p < 0.05$, one-tailed test).

Fluorine-18 fludeoxyglucose uptake for the joints of the fingers and the nail bed in psoriatic arthritis

The SUV_{max} values for the PIP joints 2–5, the DIP joints 2–5 and the nail bed for patients with PsA are reported in Table 4. The MAV was not computed, as 40% of SUV_{max} threshold was mostly at the level of the SUV values of the control or asymptomatic joints. Table 5 reports the total number of swollen, tender and PET-positive joints out of total eight joints evaluated per patient with PsA. Also reported are the SUV_{max} values for PET-positive and PET-negative joints. For the 24 joints evaluated, the SUV_{max} was significantly higher (1.96 ± 0.26) in joints that were PET positive than in those that were PET negative (1.12 ± 0.32, $p < 0.05$, two-tailed test). The number of PET-positive (6/24 or 25%) joints was the same as the number of tender (6/24 or 25%) joints, but a tad lower than the number of swollen (5/24 or 20.8%) joints. Figure 6 shows PET and CT images obtained for a typical digit with dactylitis, a hallmark of PsA, with detailed pathologies associated with the disease. The SUV_{max} in the PIP joints 2–5 across all subjects was statistically higher than that of the control joints ($p < 0.05$, one-tailed test). While remarkable spatial patterns of ^{18}F-FDG uptake as in Figure 6 were observed at the DIP, at the nail bed and along the flexor and extensor tendons in one or more digits in each patient with psA, the difference between the SUV_{max} in these areas and that of the control joints was statistically insignificant ($p = 0.10$, two-tailed test). We believe that this was a consequence of the low contrast recovery coefficients of the system for tissues of the size of tendons. We elaborate on this further in the Discussion section.

Fluorine-18 fludeoxyglucose uptake for the first carpometacarpal joint

In two patients with RA, no history or signs associated with RA or OA such as joint space narrowing, joint subluxation or erosive changes were reported for the first CMC joint on prior radiographs. For these subjects, the average SUV_{max} for the first CMC joint was 1.01. One subject had severe OA of the first CMC joint (Eaton stage III[25]) based on prior radiographs. For this subject, the SUV_{max} for the first CMC joint was 5.50 and the MAV was 6.81 cm^3. For the other two subjects, early OA (Eaton stage I/II) of the CMC joint was noted from prior radiographs and corresponded to an average SUV_{max} of 1.99 and an MAV of 2.35 cm^3. In one patient, the proximal aspect of the first metacarpal presented with erosive changes (Figure 5). In all other patients, no erosive changes to the first CMC joint which could be directly attributed to RA were noted. The high ^{18}F-FDG uptake for the first CMC joint can also be visualized in Figures 2 and 4. Table 3 reports the swelling, tenderness, PET positivity and SUV_{max} status for the first CMC joint in the five RA wrists evaluated. Although the RA subjects had a DAS 28 > 3.0, the first CMC joint was PET positive in only three out of five patients, indicating, unsurprisingly, a lack of consistency between DAS 28 and PET

Table 3. Maximum standardized uptake value (SUV_{max}) computed for the entire wrist and the first carpometacarpal (CMC) joint compared with clinical assessment and positron emission tomography (PET) positivity for patients with rheumatoid arthritis

Patient number	Wrist				First CMC joint			
	S	T	PET positivity	SUV_{max}	S	T	PET positivity	SUV_{max}
1	1	1	1	2.12	1	1	1	5.50
2	1	1	1	2.29	1	1	1	2.01
3	0	1	1	1.37	0	0	0	0.98
4	1	1	1	3.80	0	0	0	1.04
5	1	1	1	3.68	1	1	1	1.97

S, swelling; T, tenderness.
The scores for S, T and PET positivity are binary, with a 1 implying that the joint was considered positive, while 0 indicates that the joint was considered negative.

Figure 3. Fluorine-18 fludeoxyglucose (^{18}F-FDG) uptake patterns in patients with rheumatoid arthritis (RA): (a) axial section from the positron emission tomography (PET)/CT image showing elevated ^{18}F-FDG uptake in the dorsal (green arrow) [maximum standardized uptake value (SUV_{max}) = 2.93] and volar (light blue arrow) (SUV_{max} = 3.12) radiocarpal compartments. The white arrow shows a "cold" pisiform–triquetral compartment in this patient. The linear range of the PET colour scale is 26–100% of the SUV_{max}; (b) axial section from the PET/CT image of a different patient with RA showing elevated ^{18}F-FDG uptake in the pisiform–triquetral compartment (white arrow) (SUV_{max} = 3.80). The linear range of the PET colour scale is 26–77% of the SUV_{max}. For colour image see online.

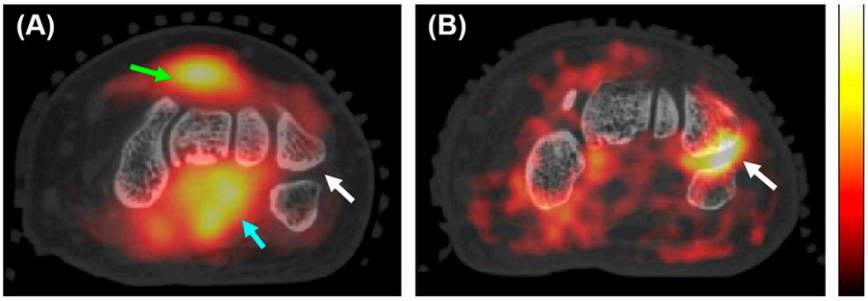

positivity for this joint. All three first CMC joints that were PET positive, however, were also positive for tenderness and swelling, while two joints that were PET negative were negative for tenderness and swelling, implying the perfect consistency of PET outcomes with tenderness and swelling for this joint.

Reliability of the maximum standardized uptake value measure

The ICC was in the excellent range, ICC = 0.99 (95% confidence interval: 0.99–1.00, $p < 0.05$),[28] indicating that evaluators had a high degree of agreement and suggesting that SUV_{max} was rated similarly across the evaluators. The high ICC also suggested that a minimal amount of measurement error was introduced by the independent evaluators. The ICC we measured for SUV_{max} in this study was similar to that reported in the published literature.[29,30]

DISCUSSION

Our results demonstrate the capability of the high-resolution extremity PET/CT system to visualize and quantify pathologies of relevance to RA and PsA in the small joints of the wrist and hand. The system provided tomographic sampling, and attenuation and scatter correction of PET data employed the co-registered CT image. Recently, the feasibility of the quad-high-density avalanche chamber nano-PET small-animal system,[31] the positron emission mammography Flex Solo II system[32,33] and the avalanche photodiode (APD)-based BrainPET system (Siemens Healthcare, Erlangen, Germany)[34] was demonstrated

Figure 4. Correlation of positron emission tomography (PET)/CT and MRI; co-registered axial sections from (a) pre-contrast T_1 weighted (T1w) scan; (b) contrast-enhanced T1W scan; (c) short tau inversion recovery (STIR) image; and (d) fluorine-18 fludeoxyglucose (^{18}F-FDG) PET overlaid on the pre-contrast T1W section. The light blue arrows indicate the dorsal radiocarpal compartment, the green arrows show the volar radiocarpal compartment with increased signal on the T1w, STIR and ^{18}F-FDG image corresponding to erosions along the volar aspects of the capitate and hamate, while the white arrows show increased fluid signal on the STIR image and elevated ^{18}F-FDG uptake for the first carpometacarpal joint. The linear range of the PET colour scale is 40–100% of the maximum standardized uptake value. For colour image see online.

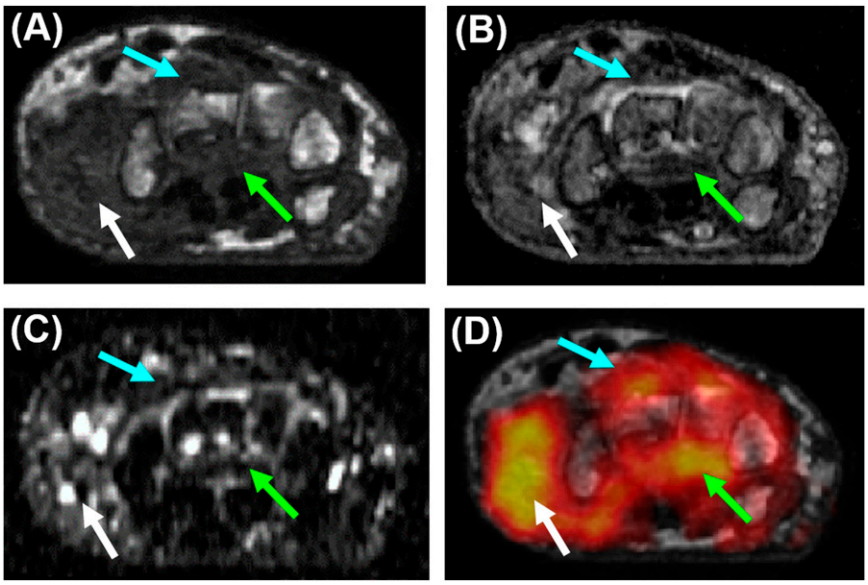

Figure 5. Elevated fluorine-18 fludeoxyglucose (^{18}F-FDG) uptake for active erosions in rheumatoid arthritis; co-registered coronal sections from (a) CT, (b) positron emission tomography (PET)/CT and (c) short tau inversion recovery MRI. The arrows indicate elevated ^{18}F-FDG uptake sites of erosive changes (white, green and light blue arrows) and in the pisiform–triquetral compartment (light brown arrows). The linear range of the PET colour scale is 40–100% of the maximum standardized uptake value. For colour image see online.

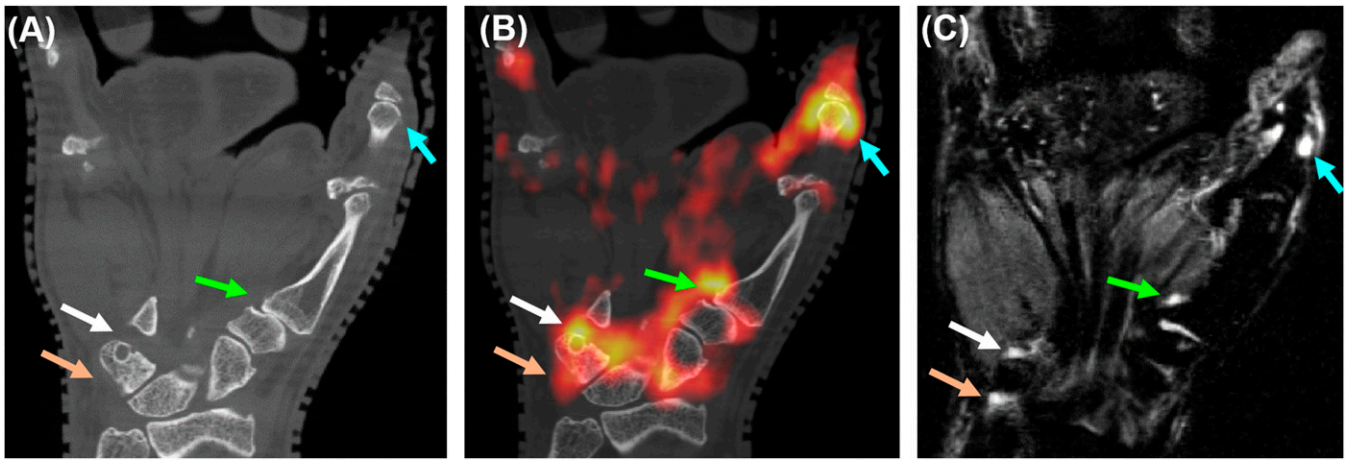

for wrist and hand arthritic imaging. These systems, however, did not have direct means for attenuation and scatter correction, and therefore radiotracer activity quantification is challenging. The PET Flex Solo II system does not provide tomographic sampling. To the best of our knowledge, this is the first study evaluating the use of fully tomographic, high-resolution, quantitative PET/CT data for elucidating the pathologies underlying RA and PsA in the wrist and hand. The quantitative data presented in our article are therefore unique and add to the growing evidence that high-resolution PET/CT may provide new information for arthritic assessment. Three areas of clinical applications of such systems could be considered: (i) early disease activity assessment and staging, owing to their ability to quantify disease activity in small joints; (ii) differential diagnosis, where radiotracer uptake patterns could reveal fundamentally different pathologies and hence allow improved therapeutic selection; and (iii) early monitoring of response to therapy, where high-resolution PET/CT could provide more sensitive and robust surrogate end points for the early assessment of arthritic drug efficacy.[35] Given that the inflammatory proliferative cascade in RA and PsA involves cellular activation, hypoxia, angiogenesis, osteoclastic and osteoblastic activity,[36] there is potential to employ targeted radiotracers[37] with high-resolution systems to further our ability to track disease.

Table 4. Maximum standardized uptake value (SUV_{max}) expressed as median (range) for the regions of interest in patients with psoriatic arthritis

Anatomical locations	SUV_{max}
PIPs 2–5	1.32 (0.92–2.35)
DIPs 2–5	1.16 (0.82–2.12)
Nail bed	1.17 (0.87–1.64)

DIP, distal interphalangeal; PIP, proximal interphalangeal.

All RA subjects in our study had a DAS 28 of >3.0 and had at least one wrist joint that was PET positive. For the RA wrist, our PET/CT images showed a significant uptake of ^{18}F-FDG in the radiocarpal and pisiform–triquetral compartments compared with control joints, which is consistent with physical examination findings. Both compartments are involved in early RA and although the two compartments are considered anatomically distinct, they seem to be functionally connected.[38] It is therefore likely that inflammatory processes in one compartment may be associated with those in the other. We found that ^{18}F-FDG uptake in the pisiform–triquetral and radiocarpal compartments was correlated and was either both high or both low. This association warrants further study. ^{18}F-FDG uptake was high in the proximity of sites of active bone erosions and was co-localized with the presence of oedema from STIR MRI. Given the importance of detecting the presence of and characterizing oedema early in RA,[39] high-resolution ^{18}F-FDG PET may complement STIR MRI by providing an assessment of the cellular activity of oedema. This aspect needs further investigation. Current European League Against Rheumatism (EULAR) guidelines for the clinical management of RA are based on MRI and ultrasound scans, but do not include PET or CT scans.[40] While MRI and ultrasound provide outstanding information regarding RA status, these modalities cannot probe the molecular and cellular activity of oedema or synovitis. The strength of PET/CT scans in this area warrants further investigation.

In PsA subjects, elevated ^{18}F-FDG uptake in the extensor and flexor tendon of the finger, at the enthesis and in the nail bed was a commonly observed pathology and correlated with clinical findings such as tendinitis, enthesitis and nail dystrophy, respectively. The pathologic process underlying nail involvement in PsA is not well understood and enthesitis is considered as the driver of this involvement.[41] The detailed visualization of the underlying inflammatory patterns at the enthesis (structures typically <3 mm) was not possible because of the spatial resolution limitations of our system. For tendons (cross-section <6 mm), we also believe that the reconstructed radiotracer

Table 5. Total number of swollen (S), tender (T) and positron emission tomography (PET)-positive joints out of a total of eight joints per patient and the average SUV_{max} for PET-positive and PET-negative joints

Patient number	Number of S	Number of T	Number of PET positive	Average SUV_{max} (PET positive)	Average SUV_{max} (PET negative)
1	1	1	1	1.91	0.94
2	3	4	4	2.10	1.38
3	1	1	1	1.46	1.11

The eight joints constitute the proximal interphalangeal joints 2–5 and the distal interphalangeal joints 2–5.

concentration was severely underestimated—for a fillable sphere of that size, our previous experiments showed that the scanner had a contrast recovery coefficient <30%.[16] Systems with a higher spatial resolution for PET are therefore needed. Ferrero et al[42] recently built a next-generation PET/CT scanner with an approximately 8 fold improvement in the volumetric spatial resolution and plan to test its performance in the arthritic population.

Elevated ^{18}F-FDG uptake was measured at the first CMC joint in patients who had radiographic signs of OA. ^{18}F-FDG uptake broadly associated with Eaton stage, but not with DAS 28. Future studies of RA or PsA using ^{18}F-FDG PET must take OA joint activity into account when estimating RA or PsA disease activity to reduce confounding.

The control ROIs we employed were drawn on the bone. We considered using other tissues, but in this patient cohort, there is a paucity of large soft-tissue structures in the wrist and hand whose ^{18}F-FDG uptake is not influenced by pathology and that could serve as control regions. We did, however, find that the SUV measures for our chosen control regions were not significantly different from the SUV measures derived in the synovial region of joints that did not present with swelling or tenderness during the clinical examination and were negative on PET.

A limitation of our study is the unavailability of ultrasound for correlating with our findings from PET/CT. Ultrasound is currently commonly employed in rheumatology clinics[43] and has demonstrated a high sensitivity for the detection of synovitis.[44] Ultrasound, however, is not able to directly interrogate the

Figure 6. Fluorine-18 fludeoxyglucose (^{18}F-FDG) uptake patterns in psoriatic arthritis dactylitis; co-registered sagittal sections from (a) CT, (b) positron emission tomography (PET) and (c) PET/CT. The light blue arrows show tenosynovitis at the proximal interphalangeal (PIP) joint, also manifested as a flexor tendon distention on the CT image [maximum standardized uptake value (SUV_{max}) = 2.35]. Green and brown arrows show elevated ^{18}F-FDG uptake at the extensor tendon enthesis at the distal phalange (SUV_{max} = 1.53) and the nail bed (SUV_{max} = 1.64), respectively, consistent with enthesitis and nail bed inflammation of this digit reported in the physical examination. For colour image see online.

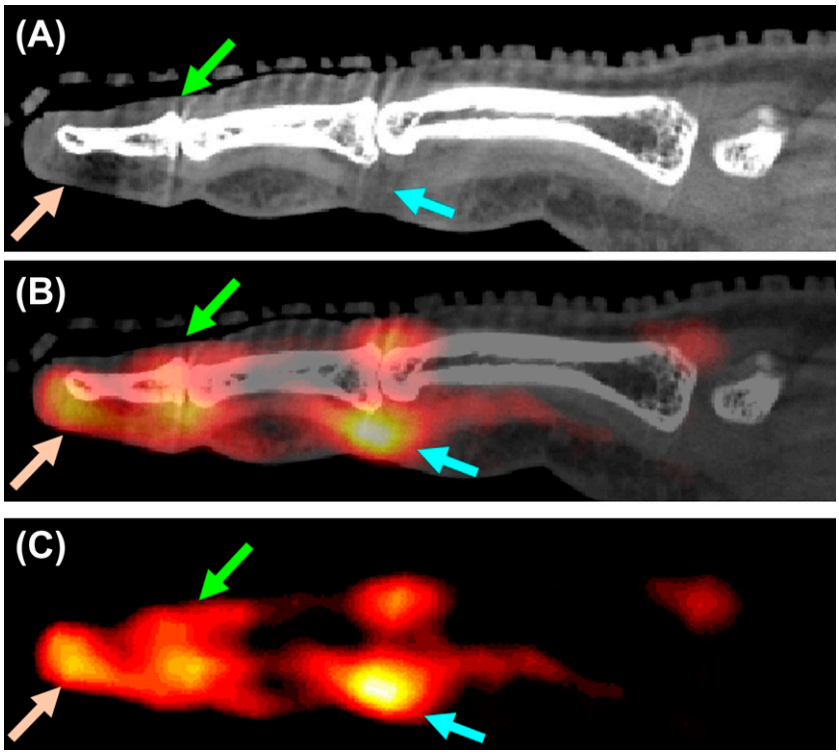

molecular activity associated with synovitis like PET/CT is able to. Therefore, studies focusing on comparing the two modalities for the wrist and finger joints are needed.

Our study had other limitations. We used approximately 85 min as our radiotracer uptake time. This choice was based on logistics associated with patient transport and positioning. An optimization of uptake time to best obtain contrast for tissues of interest needs further investigation. Dynamic PET data collection was not feasible in our system because of its step-and-shoot acquisition protocol. This limitation has been addressed in a next-generation system,[42] where investigators could optionally employ a population-based arterial input function[45] or arterial blood sampling. Kinetic parameters thus derived could reveal new knowledge about RA or PsA pathogenesis. We investigated a small number of patients who already had established RA or PsA; we did not use healthy controls, patients with low disease activity or patients who were taking biologic drugs as standard of care. This study was observational in nature and given the small sample size, only descriptive statistics and explorative statistical analyses of the imaging measures were possible. Although the measures were compared with those from the concurrently obtained MRI scan, they were not validated against ground truth tissue analysis. Given the cross-sectional nature of the study, implications of imaging findings longitudinally were unknown.

CONCLUSION

This study demonstrates that high-resolution PET/CT imaging of the wrist and hand is feasible in an RA or PsA patient cohort and is capable of providing quantifiable measures to correlate with clinical findings. These measures can be tested in future studies to determine their use in providing an improved understanding of autoimmune inflammatory arthritis *in vivo*, for evaluating disease status and activity, in determining therapeutic response and for rapidly screening targeted therapies.

ACKNOWLEDGMENTS

The authors thank Dr Michael H Buonocore, Dr Spencer L Bowen, Dr Simon R Cherry, Dr Jinyi Qi and Dr John Brock for insightful discussions regarding device instrumentation and data interpretation.

FUNDING

This study was funded by the National Institutes of Health grants 2K12 HD051958 and R03 EB015099 to AJC, R01 CA129561 to RDB, R01 EB002138 to JMB and UL1 TR000002 pilot award to RDB and AJC. The views expressed in this article are the authors' own and do not necessarily represent the views of the National Institutes of Health or the US Government.

REFERENCES

1. Firestein GS. Evolving concepts of rheumatoid arthritis. *Nature* 2003; **423**: 356–61. doi: http://dx.doi.org/10.1038/nature01661
2. Cornelius P, Marlowe M, Pekala PH. Regulation of glucose transport by tumor necrosis factor-alpha in cultured murine 3T3-L1 fibroblasts. *J Trauma* 1990; **30**(Suppl. 12): S15–20.
3. Matsui T, Nakata N, Nagai S, Nakatani A, Takahashi M, Momose T, et al. Inflammatory cytokines and hypoxia contribute to 18F-FDG uptake by cells involved in pannus formation in rheumatoid arthritis. *J Nucl Med* 2009; **50**: 920–6. doi: http://dx.doi.org/10.2967/jnumed.108.060103
4. Tse HY, Shaw MK. Autoimmunity and Disease. *Immunology, Infection, and Immunity*: American Society of Microbiology; 2004.
5. Beckers C, Ribbens C, André B, Marcelis S, Kaye O, Mathy L, et al. Assessment of disease activity in rheumatoid arthritis with (18)F-FDG PET. *J Nucl Med* 2004; **45**: 956–64.
6. Palmer WE, Rosenthal DI, Schoenberg OI, Fischman AJ, Simon LS, Rubin RH, et al. Quantification of inflammation in the wrist with gadolinium-enhanced MR imaging and PET with 2-[F-18]-fluoro-2-deoxy-D-glucose. *Radiology* 1995; **196**: 647–55. doi: http://dx.doi.org/10.1148/radiology.196.3.7644624
7. Roivainen A, Parkkola R, Yli-Kerttula T, Lehikoinen P, Viljanen T, Möttönen T, et al. Use of positron emission tomography with methyl-11C-choline and 2-18F-fluoro-2-deoxy-glucose in comparison with magnetic resonance imaging for the assessment of inflammatory proliferation of synovium. *Arthritis Rheum* 2003; **48**: 3077–84. doi: http://dx.doi.org/10.1002/art.11282
8. Nakamura H, Masuko K, Yudoh K, Kato T, Nishioka K, Sugihara T, et al. Positron emission tomography with 18F-FDG in osteoarthritic knee. *Osteoarthritis Cartilage* 2007; **15**: 673–81. doi: http://dx.doi.org/10.1016/j.joca.2006.12.010
9. Goerres GW, Forster A, Uebelhart D, Seifert B, Treyer V, Michel B, et al. F-18 FDG whole-body PET for the assessment of disease activity in patients with rheumatoid arthritis. *Clin Nucl Med* 2006; **31**: 386–90. doi: http://dx.doi.org/10.1097/01.rlu.0000222678.95218.42
10. Døhn UM, Ejbjerg BJ, Hasselquist M, Narvestad E, Møller J, Thomsen HS, et al. Detection of bone erosions in rheumatoid arthritis wrist joints with magnetic resonance imaging, computed tomography and radiography. *Arthritis Res Ther* 2008; **10**: R25. doi: http://dx.doi.org/10.1186/ar2378
11. Scott DL, Coulton BL, Popert AJ. Long term progression of joint damage in rheumatoid arthritis. *Ann Rheum Dis* 1986; **45**: 373–8. doi: http://dx.doi.org/10.1136/ard.45.5.373
12. Sterne E Jr, Schneider B. Psoriatic arthritis. *Ann Intern Med* 1953; **38**: 512–22. doi: http://dx.doi.org/10.7326/0003-4819-38-3-512
13. Elzinga EH, van der Laken CJ, Comans EF, Lammertsma AA, Dijkmans BA, Voskuyl AE. 2-Deoxy-2-[F-18]fluoro-D-glucose joint uptake on positron emission tomography images: rheumatoid arthritis *versus* osteoarthritis. *Mol Imaging Biol* 2007; **9**: 357–60. doi: http://dx.doi.org/10.1007/s11307-007-0113-4
14. MacDonald L, Edwards J, Lewellen T, Haseley D, Rogers J, Kinahan P. Clinical imaging characteristics of the positron emission mammography camera: PEM Flex Solo II. *J Nucl Med* 2009; **50**: 1666–75. doi: http://dx.doi.org/10.2967/jnumed.109.064345
15. Wu Y, Bowen SL, Yang K, Packard N, Fu L, Burkett G, et al. PET characteristics of a dedicated breast PET/CT scanner prototype. *Phys Med Biol* 2009; **54**: 4273–87. doi: http://dx.doi.org/10.1088/0031-9155/54/13/020
16. Bowen SL, Ferrero A, Badawi RD. Quantification with a dedicated breast PET/CT scanner. *Med Phys* 2012; **39**: 2694–707. doi: http://dx.doi.org/10.1118/1.3703593

17. Felson DT, Anderson JJ, Boers M, Bombardier C, Furst D, Goldsmith C, et al. American College of Rheumatology. Preliminary definition of improvement in rheumatoid arthritis. *Arthritis Rheum* 1995; **38**: 727–35. doi: http://dx.doi.org/10.1002/art.1780380602
18. Taylor W, Gladman D, Helliwell P, Marchesoni A, Mease P, Mielants H, et al. Classification criteria for psoriatic arthritis: development of new criteria from a large international study. *Arthritis Rheum* 2006; **54**: 2665–73. doi: http://dx.doi.org/10.1002/art.21972
19. Wright V, Moll JM. Psoriatic arthritis. *Bull Rheum Dis* 1971; **21**: 627–32.
20. Fransen J, van Riel PL. The Disease Activity Score and the EULAR response criteria. *Clin Exp Rheumatol* 2005; **23**(5 Suppl. 39): S93–9.
21. Chaudhari AJ, Burkett GW, Bowen SL, Harse R, Packard NJ, Stern RL, et al, eds. Multimodality high resolution wrist imaging for monitoring response to therapy in rheumatoid arthritis: Instrumentation and techniques. *IEEE Nuclear Science Symposium Conference Record*: IEEE; 2008.
22. Boone JM, Kwan AL, Yang K, Burkett GW, Lindfors KK, Nelson TR. Computed tomography for imaging the breast. *J Mammary Gland Biol Neoplasia* 2006; **11**: 103–11. doi: http://dx.doi.org/10.1007/s10911-006-9017-1
23. Nestle U, Kremp S, Schaefer-Schuler A, Sebastian-Welsch C, Hellwig D, Rübe C, et al. Comparison of different methods for delineation of 18F-FDG PET-positive tissue for target volume definition in radiotherapy of patients with non-small cell lung cancer. *J Nucl Med* 2005; **46**: 1342–8.
24. van der Heijde D. How to read radiographs according to the Sharp/van der Heijde method. *J Rheumatol* 1999; **26**: 743–5.
25. Eaton RG, Glickel SZ. Trapeziometacarpal osteoarthritis. Staging as a rationale for treatment. *Hand Clin* 1987; **3**: 455–71.
26. Ostergaard M, Edmonds J, McQueen F, Peterfy C, Lassere M, Ejbjerg B, et al. An introduction to the EULAR-OMERACT rheumatoid arthritis MRI reference image atlas. *Ann Rheum Dis* 2005; **64**(Suppl. 1): i3–7. doi: http://dx.doi.org/10.1136/ard.2004.031773
27. McGraw KO, Wong SP. Forming inferences about some intraclass correlation coefficients. *Psychol Methods* 1996; **1**: 30–46. doi: http://dx.doi.org/10.1037/1082-989X.1.1.30
28. Cicchetti DV. Guidelines, criteria, and rules of thumb for evaluating normed and standardized assessment instruments in psychology. *Psychol Assess* 1994; **6**: 284. doi: http://dx.doi.org/10.1037/1040-3590.6.4.284
29. Huang Y-E, Chen C-F, Huang Y-J, Konda SD, Appelbaum DE, Pu Y. Interobserver variability among measurements of the maximum and mean standardized uptake values on (18)F-FDG PET/CT and measurements of tumor size on diagnostic CT in patients with pulmonary tumors. *Acta Radiol* 2010; **51**: 782–8. doi: http://dx.doi.org/10.3109/02841851.2010.497772
30. Tixier F, Hatt M, Le Rest CC, Le Pogam A, Corcos L, Visvikis D. Reproducibility of tumor uptake heterogeneity characterization through textural feature analysis in 18F-FDG PET. *J Nucl Med* 2012; **53**: 693–700. doi: http://dx.doi.org/10.2967/jnumed.111.099127
31. Tan AL, Tanner SF, Waller ML, Hensor EM, Burns A, Jeavons AP, et al. High-resolution [18F]fluoride positron emission tomography of the distal interphalangeal joint in psoriatic arthritis—a bone-enthesis-nail complex. *Rheumatology (Oxford)* 2013; **52**: 898–904. doi: http://dx.doi.org/10.1093/rheumatology/kes384
32. Rahim S, Mawlawi O, Taylor S, Millican R, Swanston NM, Brown JE, et al. Is imaging the extremities with PEM feasible? A novel application for a high-resolution positron emission scanner. *Clin Imaging* 2014; **38**: 307–13. doi: http://dx.doi.org/10.1016/j.clinimag.2013.11.013
33. Mhlanga JC, Carrino JA, Lodge M, Wang H, Wahl RL. 18F-FDG PET of the hands with a dedicated high-resolution PEM system (arthro-PET): correlation with PET/CT, radiography and clinical parameters. *Eur J Nucl Med Mol Imaging* 2014; **41**: 2337–45. doi: http://dx.doi.org/10.1007/s00259-014-2856-x
34. Miese F, Scherer A, Ostendorf B, Heinzel A, Lanzman RS, Kröpil P, et al. Hybrid 18F-FDG PET-MRI of the hand in rheumatoid arthritis: initial results. *Clin Rheumatol* 2011; **30**: 1247–50. doi: http://dx.doi.org/10.1007/s10067-011-1777-3
35. Chaudhari AJ, Bowen SL, Burkett GW, Packard NJ, Godinez F, Joshi AA, et al. High-resolution (18)F-FDG PET with MRI for monitoring response to treatment in rheumatoid arthritis. *Eur J Nucl Med Mol Imaging* 2010; **37**: 1047. doi: http://dx.doi.org/10.1007/s00259-009-1364-x
36. McInnes IB, Schett G. The pathogenesis of rheumatoid arthritis. *N Engl J Med* 2011; **365**: 2205–19. doi: http://dx.doi.org/10.1056/NEJMra1004965
37. Put S, Westhovens R, Lahoutte T, Matthys P. Molecular imaging of rheumatoid arthritis: emerging markers, tools, and techniques. *Arthritis Res Ther* 2014; **16**: 208. doi: http://dx.doi.org/10.1186/ar4542
38. Arya AP, Kulshreshtha R, Kakarala GK, Singh R, Compson JP. Visualisation of the piso-triquetral joint through standard portals for arthroscopy of the wrist: a clinical and anatomical study. *J Bone Joint Surg Br* 2007; **89**: 202–5. doi: http://dx.doi.org/10.1302/0301-620X.89B2.18540
39. Jimenez-Boj E, Nöbauer-Huhmann I, Hanslik-Schnabel B, Dorotka R, Wanivenhaus AH, Kainberger F, et al. Bone erosions and bone marrow edema as defined by magnetic resonance imaging reflect true bone marrow inflammation in rheumatoid arthritis. *Arthritis Rheum* 2007; **56**: 1118–24. doi: http://dx.doi.org/10.1002/art.22496
40. Colebatch AN, Edwards CJ, Østergaard M, van der Heijde D, Balint PV, D'Agostino MA, et al. EULAR recommendations for the use of imaging of the joints in the clinical management of rheumatoid arthritis. *Ann Rheum Dis* 2013; **72**: 804–14. doi: http://dx.doi.org/10.1136/annrheumdis-2012-203158
41. Tan AL, Fukuba E, Halliday NA, Tanner SF, Emery P, McGonagle D. High-resolution MRI assessment of dactylitis in psoriatic arthritis shows flexor tendon pulley and sheath-related enthesitis. *Ann Rheum Dis* 2014; **74**: 185–9. doi: http://dx.doi.org/10.1136/annrheumdis-2014-205839.
42. Ferrero A, Peng Q, Burkett GW Jr, Sumanasena B, Moses WW, Badawi RD. Preliminary performance characterization of DbPET2.1, a PET scanner dedicated to the imaging of the breast and extremities. *Biomed Phys Eng Express* 2015; **1**: 015202.
43. Larché M, Lyddell C, Bykerk V, Dhindsa N, Adams K, Stein M, et al. Utilization of musculoskeletal ultrasound in daily rheumatology practice and research. *Can Rheumatol Assoc J* 2013; **23**: 25–8.
44. Nakagomi D, Ikeda K, Okubo A, Iwamoto T, Sanayama Y, Takahashi K, et al. Ultrasound can improve the accuracy of the 2010 American College of Rheumatology/European League against rheumatism classification criteria for rheumatoid arthritis to predict the requirement for methotrexate treatment. *Arthritis Rheum* 2013; **65**: 890–8. doi: http://dx.doi.org/10.1002/art.37848
45. Takikawa S, Dhawan V, Spetsieris P, Robeson W, Chaly T, Dahl R, et al. Noninvasive quantitative fluorodeoxyglucose PET studies with an estimated input function derived from a population-based arterial blood curve. *Radiology* 1993; **188**: 131–6. doi: http://dx.doi.org/10.1148/radiology.188.1.8511286